PROCEEDINGS OF SCIENCE

# The Pierre Auger Observatory: latest results and future perspectives

**Federico Sánchez**[a,*] **on behalf of the Pierre Auger Collaboration**[b]

[a] *Instituto de Tecnologías en Detección y Astropartículas (CNEA, CONICET, UNSAM), Av. General Paz 1555 (B1630KNA) San Martín, Buenos Aires, Argentina*

[b] *Observatorio Pierre Auger, Av. San Martín Norte 304, 5613 Malargüe, Argentina*

*Full author list:* *https://www.auger.org/archive/authors_2022_7.html*

*E-mail:* spokespersons@auger.org

The Pierre Auger Observatory, in the south of Mendoza province (Argentina), is the largest facility in the world to observe ultra-high-energy cosmic rays (UHECR) and has been taking data for more than fifteen years. It is designed to simultaneously detect the longitudinal development of the extensive air showers in the atmosphere and measure of particles' densities at ground level. This hybrid technique allowed us to produce results with unprecedented precision. In this talk, we report on the latest updates on the spectrum, mass composition and arrival directions of cosmic rays in the range of $10^{16.5}$ eV to $10^{20.0}$ eV.

*41st International Conference on High Energy Physics - ICHEP2022*
*6-13 July, 2022*
*Bologna, Italy*

*Speaker





PoS(ICHEP2022)107

## 1. Introduction

Unveiling the origin of Ultra-High Energy Cosmic Rays (UHECR) remains an important and still complicated task in the field of astroparticle physics. In the past fifteen years, the measurements of the Pierre Auger Observatory have shed light on their energy spectrum, chemical composition and arrival directions at Earth, leading to great advances in the field. Nevertheless, the emerged landscape is much more complex than previously expected, and we are still lacking a comprehensive model to properly explain the mechanism that energizes these particles, their abundances, their energies and, finally, the location of their sources. Moreover, to further complicate our interpretation of data, we have to rely on hadronic interaction models that have to be extrapolated to much higher energies than those at which they were tested in modern accelerators. A discrepancy has

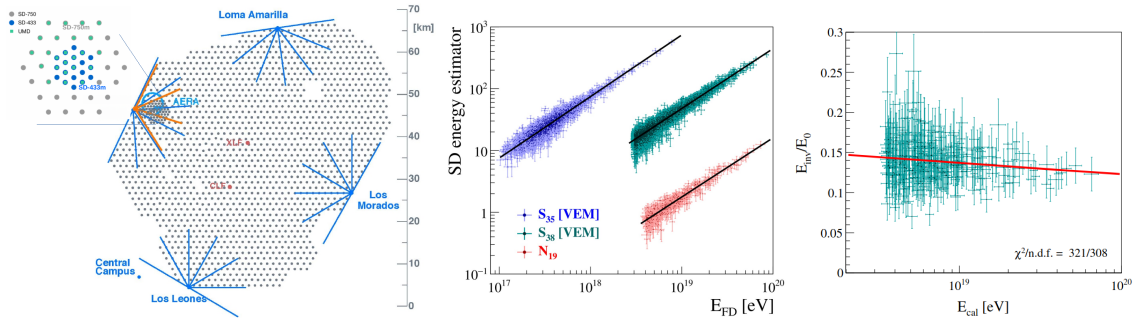


**Figure 1:** Layout of the Pierre Auger Observatory: SD-1500 over 3000 km$^2$ (gray dots), SD-750 over 23.5 km$^2$ (inset, gray dots) and SD-433 over 1.9 km$^2$ (inset, blue dots). The Underground Muon Detector (UMD) of AMIGA and the AERA enhancements are also indicated (left). Calibration functions of the SD energy estimators to the energies reconstructed by the FD: $S_{38}$ and $N_{19}$ for the array of 1500 m using events between $0° - 60°$ and $60° - 80°$, respectively; and $S_{35}$ for the array of 750 m using events between $0° - 60°$ (center). Data-driven parametrization of the invisible energy (right).

been measured between the predicted muonic component of extensive air showers and UHECR observations. Even if this tension hinders data comprehension, it might also contribute to increase our knowledge of the standard model of particle physics and, possibly, to explore effects beyond it. The Pierre Auger Observatory consists of a surface detector of about 1660 water-Cherenkov stations distributed in a triangular grid. The largest array, with 1500 m spacing (SD-1500), covering a total area of 3000 km$^2$, has embedded two denser arrays with spacings of 750 m (SD-750) and 433 m (SD-433) over areas of 23.5 km$^2$ and 1.9 km$^2$, respectively. The SD system is overlooked by 24 air-fluorescence telescopes (FD) with a field-of-view (FoV) between $0° - 30°$ and three within $30° - 60°$ (named **H**igh-**E**levation **A**uger **T**elescopes, HEAT). All these FD units are grouped at four sites overlooking the whole SD array as indicated in Fig. 1. Additionally, as part of the **A**uger **M**uon and **I**nfill for the **G**round **A**rray (AMIGA) [1] and the **A**uger **E**ngineering **R**adio **A**rray (AERA) [2] enhancements, prototypes of an underground muon detector (UMD) and a radio detector (RD) were developed in the region of the SD-750 array. The graded array system allows the Auger Observatory to measure UHECR-induced air showers from $10^{16.5}$ eV up to the highest energies. The combination of the SD and the FD observations of the same events, the so-called *hybrid* technique, allows a drastic improvement of the systematics and a better resolution. The longitudinal development of the extensive air showers (EAS) is observed by the FD for a fraction of about 15% of the total number of

events, corresponding to those arriving during moonless nights. In this way, the calorimetric energy deposited by secondary particles in the atmosphere can be measured. When the unobservable (or *invisible*) energy carried-on mostly by muons and neutrinos, is taken into account, the energy of the primary cosmic ray inducing the shower can be reconstructed. It is worth noticing that the recently data-driven parametrization of the invisible energy was found to be 10%-15% higher than purely Monte-Carlo predictions previously used. For this subset of hybrid data, the correlation between the particle density at the ground (measured at a fixed and optimal distance depending on the SD array used) and the FD reconstructed energy can be exploited to obtain a calibration for all the SD events in an almost model-independent way. The FD energy resolution amounts to about 8%, while the overall systematic uncertainty on the energy scale is 14% [3]. The calibration curves, together with the data-driven parametrization of the invisible energy, are shown in the center and right-most panel of Fig. 1 [4, 5].

## 2. Energy spectrum

The measurements of the energy spectrum with five independent reconstruction methods are shown in Fig. 2 (left). Those made with the 1500 m array using events with zenith angles in two distinct ranges ($0° - 60°$, the *vertical* events and $60° - 80°$, the *inclined* events), those with at least one SD station was triggered jointly to an FD observation (the *hybrid events*), the vertical events triggering the 750 m SD array and the FD events dominated by Cherenkov light are used to cover an energy range from $6 \times 10^{15}$ eV to above $10^{20}$ eV. The combined measurements into a single estimate of the spectrum through a forward–folding approach [6] are shown in the right panel of Fig. 2. The so-called *ankle* and the flux suppression are clearly visible at $(4.9 \pm 0.1 \pm 0.8) \times 10^{18}$ eV and $(4.7 \pm 0.3 \pm 0.6) \times 10^{19}$ eV. A feature so far unobserved, dubbed the *instep*, has been clearly

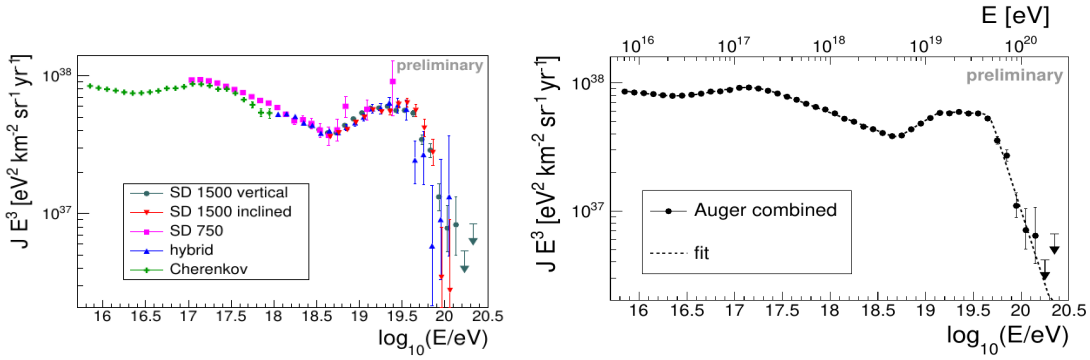


**Figure 2:** Intensity of cosmic rays multiplied by $E^3$ estimated using five different techniques (left) and combined energy spectrum together with the fit function (dashed line).

identified at $1.4 \times 10^{19}$ eV. The energy at which the integral spectrum drops by a factor of two below what would be expected with no steepening is $E_{1/2} = (2.3 \pm 4) \times 10^{19}$ eV.

## 3. Composition

The first two moments of the depth of shower maximum distributions are shown in the left and central panels of Fig. 3. The observed evolution of the mean value of $X_{\max}$ with en-

ergy shows a clear break just below the energy of the ankle, around $10^{18.32\pm0.03}$ eV. The rate of change is from 77 g/cm$^2$/decade to 26 g/cm$^2$/decade while a constant composition would have had ~60 g/cm$^2$/decade. The comparison with the predictions from hadronic interaction models tuned to

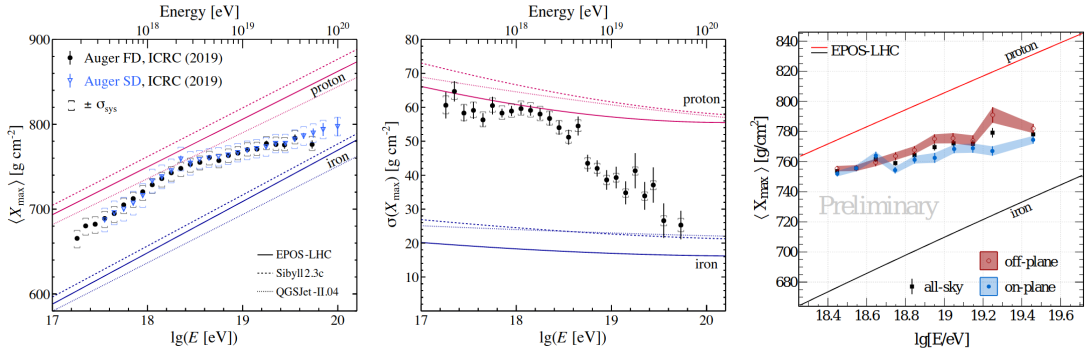


**Figure 3:** The average values of $X_{\rm max}$ as a function of energy (left panel) and its standard deviation (central panel). On the right panel, the elongation rate is separated for events arriving within $|b| < 30°$ of the Galactic plane (*on-plane*) and those with higher latitudes (*off-plane*).

the most recent Large Hadron Collider (LHC) results are also shown in the figure. Assuming a pure primary composition, the change in the elongation rate of $X_{\rm max}$ indicates a change towards lighter elements up to the break, while above, there is an increase in the average mass. The results are obtained by analyzing two independent data sets: in black, the direct measurement of $X_{\rm max}$ by the FD, in blue, the SD result using the rise-time of the signal in the water-Cherenkov stations as a proxy of the primary mass. It is worth noting that this latter sample allows us to extend the composition measurements up to higher energies, although at the expense of larger systematic uncertainties. This findings are also confirmed by means of the standard deviations of $X_{\rm max}$ shown in the right panel of the same figure. The large values of $\sigma(X_{\rm max})$ below the energy of the break can be interpreted as coming from either light or mixed primaries, whereas the subsequent decrease would correspond to a purer intermediate to heavy composition. A completely independent measurement of the $X_{\rm max}$ distributions was recently obtained by exploiting the AERA radio array, confirming the previous conclusion [7].

A recent analysis has tested the hypothesis of an anisotropy lying along the Galactic plane, which depends on the mass of primary cosmic rays [8]. For this study, 14 years of available data are split into *on-* and *off*-plane regions using the Galactic latitude of each event to form two distributions in $X_{\rm max}$. The optimal energy and latitude, found in scanning data, were $E = 10^{18.7}$ eV and $|b| = 30°$ respectively. This analysis suggests that the average composition of UHECRs appears to be heavier below $|b| = 30°$, as shown in the right panels of Fig. 3.

## 4. Combining spectrum and composition

A combined fit of a simple astrophysical model of UHECR sources to both the energy spectrum and mass composition data was exploited to investigate the constraining power of the collected data on the source properties. Considering a simple astrophysical scenario of stationary and uniform sources in a co-moving volume, we have taken into account several nuclear components injected at

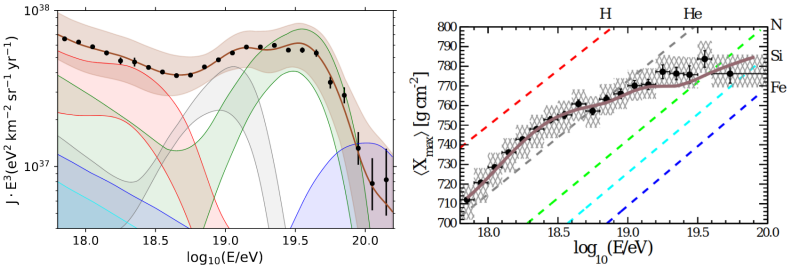


**Figure 4:** The energy spectrum and the relative abundances at the top of atmosphere (left). The shaded areas indicate the combined effect of systematic uncertainties. Colors indicate mass groups: $A = 1$ (red), $2 \leq A \leq 4$ (gray), $5 \leq A \leq 22$ (green), $23 \leq A \leq 38$ (cyan), $A \geq 39$ (blue). On the right panel, the best fit to $X_{\rm max}$ data.

the sources with a power-law spectrum and with the maximal energy of the sources modeled with an exponential cut-off. A good description of our data is obtained by considering two extragalactic components. Above the ankle, medium mass elements are escaping from the sources with a very hard energy spectrum and a rather low rigidity cut-off; the flux suppression appears to be mainly due to source exhaustion rather than to propagation effects as shown in Fig. 4. At lower energies, an additional light or light-to-intermediate very soft extragalactic component is needed. But a similar result might also be obtained when this component is taken as an extragalactic proton-only one, and a medium-mass Galactic contribution is added.

## 5. Arrival direction distributions

The Pierre Auger Observatory can cover 85% of the sky observing events with zenith angles up to 80°. In this way, it was possible to determine, with high significance, an anisotropy in the cosmic-ray arrival direction distribution at energies above 8 EeV[10], as can be seen in the left panel of Fig. 5. The measured anisotropy has a large angular scale characteristic showing a dipolar pattern with an amplitude of about 7%, with the reconstructed dipole pointing about 115° away from the direction of the Galactic center. This direction provides a clear indication in support of

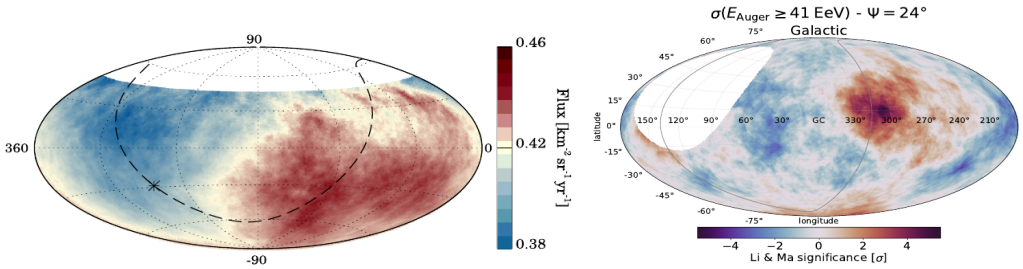


**Figure 5:** Map of dipole distribution of arrival directions of cosmic rays with energy above 8 EeV in equatorial coordinates (left) and local Li-Ma significance at energies above 41 EeV, within a top-hat search angle of 24°, in Galactic coordinates (right).

the extragalactic origin of the cosmic rays at these energies. Considering several energy bins above 8 EeV, the dipole amplitude is found to increase with energy, and the direction of the fitted dipole in

all bins lies not far from the direction of the outer spiral arm of the Galaxy. At energies below 8 EeV, no significant anisotropies were observed, so that relevant upper bounds on the equatorial dipole amplitudes were set down to energies of 0.03 EeV, and interestingly, the right ascension phase of the flux modulations below about 1 EeV is not far from the right ascension of the Galactic center. Hints of anisotropies at intermediate angular scales, of the order of 20°, have been obtained at energies above about 40 EeV (right panel of Fig. 5), with the main excess lying around the direction towards the nearby radiogalaxy Centaurus A [10]. This radiogalaxy then provides a possible candidate source of UHECR, although other potential sources are located in the same region of the sky, such as the starburst galaxies NGC4945 and M83.

## 6. Future perspectives

The Pierre Auger Observatory is, at present, undergoing an upgrade, dubbed *AugerPrime*. The underlying idea is to improve the sensitivity to mass composition observables. For each Water-Cherenkov detector, AugerPrime foresees an additional $4\,\mathrm{m}^2$ scintillators on top, an additional small-area photomultiplier tube, and an additional radio antenna to observe the radio emission from the electromagnetic component of the shower. The current electronics will be upgraded to increase the sampling frequency of the signals by a factor 3. Finally, the SD-750 and the SD-433 will be equipped with underground scintillators to provide a direct measurement of the muonic component of the extensive air showers. The aim of AugerPrime is to provide a cleaner separation between the electromagnetic and muonic components of the showers and, therefore, to obtain composition information on an event-by-event basis.

## References

[1] A. Botti, Proc. $37^{th}$ Int. Cosmic Ray Conf., Berlin (Germany) (2021), PoS(ICRC2021) 233.

[2] T. Huege, *EPJ Web of Conferences* **210**, 05011 (2019).

[3] B. Dawson, Proc. $36^{th}$ Int. Cosmic Ray Conf., Madison (USA), PoS(ICRC2019) 231.

[4] A. Aab et al. [Pierre Auger Coll.], *Phys. Rev. D* **100** (2019).

[5] V. Novotny, Proc. $37^{th}$ Int. Cosmic Ray Conf., Berlin (Germany) (2021), PoS(ICRC2021) 324.

[6] A. Aab et al. [Pierre Auger Coll.], *Eur. Phys. J. C* **81** (2021) 966.

[7] B. Pont, Proc. $37^{th}$ Int. Cosmic Ray Conf., Berlin (Germany) (2021), PoS(ICRC2021) 387.

[8] E. Mayotte, Proc. $37^{th}$ Int. Cosmic Ray Conf., Berlin (Germany) (2021), PoS(ICRC2021) 321.

[9] A. Aab et al. [Pierre Auger Coll.], *The Astrophysical Journal* **864** (2018) 4.

[10] P. Abreu et al. [Pierre Auger Coll.], *The Astrophysical Journal* **935** (2022) 170.